ChemComm

Chemical Communications

www.rsc.org/chemcomm

Volume 48 | Number 49 | 21 June 2012 | Pages 6057–6188

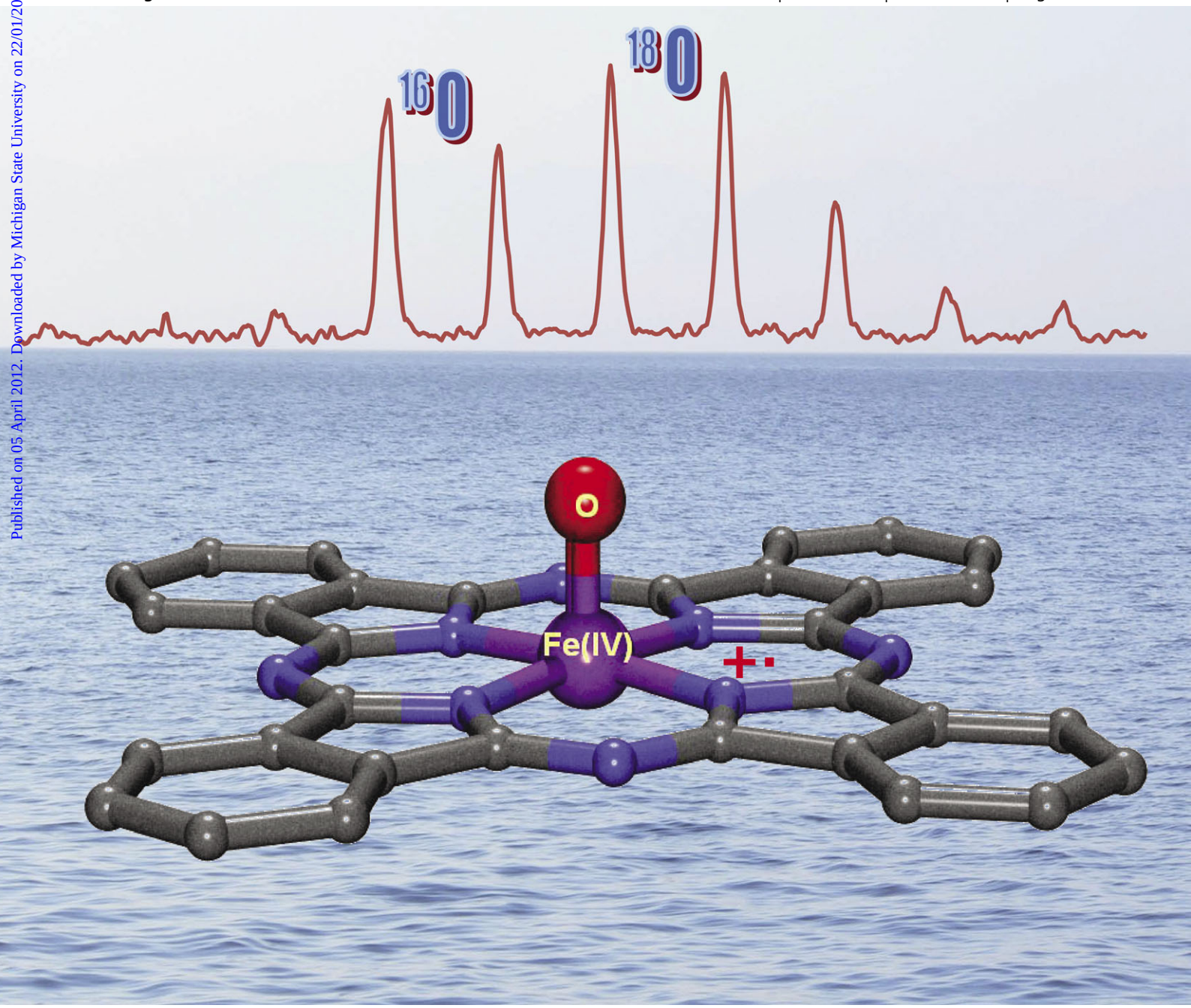

ISSN 1359-7345

RSC Publishing

COMMUNICATION

A. B. Sorokin *et al.*

Generation and characterization of high-valent iron oxo phthalocyanines

ChemComm

This article is part of the

Porphyrins & Phthalocyanines

web themed issue

Guest editors: Jonathan Sessler, Penny Brothers and Chang-Hee Lee

All articles in this issue will be gathered together online at
www.rsc.org/porphyrins

ChemComm

View Article Online
Dynamic Article Links

Cite this: *Chem. Commun.*, 2012, **48**, 6088–6090

www.rsc.org/chemcomm

COMMUNICATION

Generation and characterization of high-valent iron oxo phthalocyanines†‡

Pavel Afanasiev,*[a] Evgeny V. Kudrik,[ab] Florian Albrieux,[c] Valérie Briois,[d] Oskar I. Koifman[b] and Alexander B. Sorokin*[a]

Received 15th March 2012, Accepted 5th April 2012
DOI: 10.1039/c2cc31917a

The first high-valent iron oxo complex on the phthalocyanine platform has been prepared from iron tetra-*tert*-butyl-phthalocyanine and *m*-chloroperbenzoic acid and characterized by low temperature UV–vis, cryospray MS, EPR, X-ray absorption and high resolution X-ray emission methods.

Among the metal macrocyclic complexes used for bio-inspired catalytic oxidation, phthalocyanines are probably the most available in terms of the simple preparation, large accessible amounts and their low price.[1] They are widely used as oxidation catalysts,[2] *e.g.* in a large scale industrial Merox process.[3] Despite the great interest in phthalocyanine complexes for catalytic oxidation including industrial applications, the mechanistic aspects of their chemistry are still under-developed, especially identification and characterization of the active species.[2a] While high-valent iron oxo species on the porphyrin,[4] corrole,[5] and non-heme[6] platforms have been prepared at low temperatures and characterized, the corresponding mononuclear phthalocyanine species has often been postulated as active species, but has never been described. Only in the particular case of binuclear *N*-bridged phthalocyanines several high-valent diiron oxo species have been detected.[7] Since the catalytic performance of the complexes is closely associated to the properties of the transient active species, preparation and spectroscopic characterization of the elusive high-valent iron oxo species is of great interest.[4–6] In this context, recent capture and characterization of the long-sought cytochrome P-450 compound I intermediate is a significant achievement.[8] Here we report on the first preparation and characterization of a Fe(IV) oxo complex supported by a phthalocyanine ligand.

The reaction of tetra-*tert*-butylphthalocyanine iron chloride, (Pc^tBu_4)FeCl, and *m*-chloroperbenzoic acid (*m*-CPBA, active oxygen donor) was studied using UV–vis spectroscopy at −45 to −80 °C using several solvents (CH_2Cl_2, CH_3CN–CH_2Cl_2 mixtures and acetone). Acetone was found to be the most suitable solvent providing clear spectral changes and sufficient stability of formed species. Upon addition of 3 equiv. *m*-CPBA to the green solution of (Pc^tBu_4)FeCl in acetone at −60 °C an (Pc^tBu_4)Fe-*m*-CPBA intermediate with $\lambda = 634$ nm was rapidly formed (Fig. 1). This intermediate gradually generated a pink species with isobestic points at 603 and 662 nm and broad absorption bands at 529, 629 and 667 nm (Fig. 1). These UV–vis features are consistent with the formation of the phthalocyanine cation radical.[7d,9] The EPR spectrum of this pink intermediate exhibited a broad signal at $g = 2.01$ which suggests the presence of $S = 1/2$ species. These results are consistent with the presence of Fe(IV) sites and the unpaired electron centred on the phthalocyanine core (*vide infra*).

The formation of new species upon addition of *m*-CPBA was evidenced by cryospray mass-spectrometry. Previously we used this method for the detection of oxo and hydroperoxo diiron phthalocyanine species.[7a] A 10^{-6} M (Pc^tBu_4)FeCl solution was incubated with 10 equiv. *m*-CPBA in acetone at −75 °C for 2 min and cryospray MS analysis was rapidly

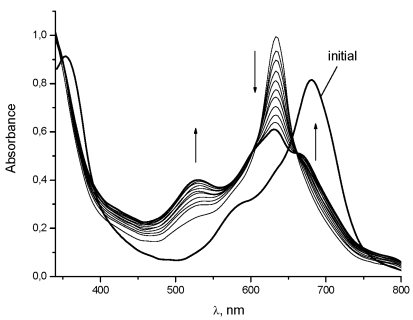

Fig. 1 UV–vis spectral changes upon addition of 3 equiv. *m*-CPBA to 1.7×10^{-5} M (Pc^tBu_4)FeCl solution in acetone at −60 °C. Spectra were recorded after 30 s intervals.

[a] *Institut de Recherches sur la Catalyse et l'Environnement de Lyon (IRCELYON), UMR 5256, CNRS-Université Lyon, 2, av. A. Einstein, 69626 Villeurbanne Cedex, France. E-mail: alexander.sorokin@ircelyon.univ-lyon1.fr, pavel.afanasiev@ircelyon.univ-lyon1.fr; Fax: +33 472445399; Tel: +33 472445337*
[b] *Institute of Macroheterocyclic Compounds, Ivanovo State University of Chemistry and Technology, 7, av. F. Engels, 153000, Ivanovo, Russia*
[c] *Université Lyon 1, UMR 5246, Centre Commun de Spectrométrie de Masse, 43 bd du 11 Novembre 1918, 69622 Villeurbanne Cedex, France*
[d] *Synchrotron Soleil, L'orme des merisiers, St-Aubin, 91192 Gif-sur-Yvette, France*

† This article is part of the *ChemComm* 'Porphyrins and phthalocyanines' web themed issue.

‡ Electronic supplementary information (ESI) available: Experimental conditions and procedures, DFT details, ESI-MS, EPR, EXAFS, XANES and XES data. See DOI: 10.1039/c2cc31917a

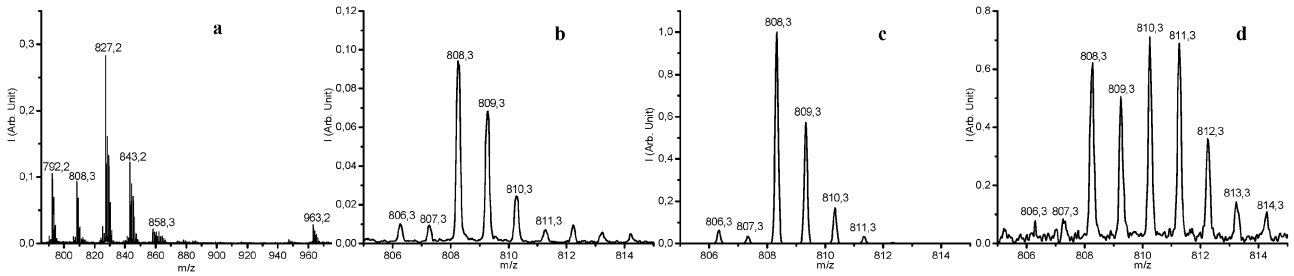

Fig. 2 Positive CSI-MS spectrum of $[(Pc^tBu_4)Fe^{IV}{=}O(Cl)]^+$; (b) an experimental isotope distribution pattern of the $[(Pc^tBu_4)Fe^{IV}{=}O]^+$ molecular cluster peak; (c) a calculated isotope distribution pattern for $C_{48}H_{48}N_8Fe_1O_1$; (d) after addition of 40 μL of $H_2{}^{18}O$ per 1 mL of 10^{-6} M complex solution.

performed at −20 °C in the positive detection mode. Along with the signal of the starting complex at m/z = 792.3 (for $[(Pc^tBu_4)Fe]^+$) a small signal at m/z = 963.2 due to peroxo complex $(Pc^tBu_4)Fe$–mCPBA was detected (Fig. 2). Most importantly, the strong signals at m/z = 808.3 and m/z = 843.2 corresponding to $[(Pc^tBu_4)Fe{=}O]^+$ and $[(Pc^tBu_4)Fe{=}O(Cl)]^+$, respectively, were observed. The latter signal could result from oxo species after the loss of one electron under MS analysis conditions. The prominent signal at m/z = 827.2 can be due to $[(Pc^tBu_4)Fe{=}O(Cl){-}O]^+$ fragmentation or due to the initial $(Pc^tBu_4)FeCl$ complex after the loss of one electron under MS analysis conditions. Thus, cryospray MS data agree with low temperature UV–vis and EPR data and the following mechanism of formation of the Fe(IV) oxo species and its formulation can be proposed (Scheme 1).

It is well established that high valent metal oxo species are amenable to exchange the oxo ligand with labelled $H_2{}^{18}O$.[10] In order to check this possibility 20 μL of $H_2{}^{18}O$ (95.4% isotopic purity) in 80 μL of acetone were added to $(Pc^tBu_4)Fe{=}O(Cl)$ acetone solution (10^{-6} M, 1 mL) at −75 °C. After 3 min incubation the resulting solution was analyzed under the same cryospray MS analysis conditions. The strong increase of the signal at m/z = 810.3 indicated oxygen exchange of Fe(IV)=O with labelled water. After correction of the intensity of m/z = 810.3 in the initial spectrum before $H_2{}^{18}O$ addition, the isotopic composition of the oxo species was calculated to be 65% $[(Pc^tBu_4)Fe{=}{}^{16}O]^+$ and 35% $[(Pc^tBu_4)Fe{=}{}^{18}O]^+$ which didn't change after further 3 min incubation at −75 °C. After the second 20 μL $H_2{}^{18}O$ addition the content of the labelled oxo species $[(Pc^tBu_4)Fe{=}{}^{18}O]^+$ reached 49%. This implies rapid isotopic exchange of the oxo ligand.

To gain further insight into the properties of the oxo complex, we carried out density functional theory (DFT) and time-dependent DFT (TDDFT) calculations, using the program ORCA, version 2.8.[11a] The goal was to predict the structure of oxo-species and to simulate their Fe K edge X-ray absorption spectra. As shown in the papers by Neese and colleagues, DFT calculations using BP86 functional and TZVP/CP(PPP) basis allow reproducing the features observed in the X-ray core-level emission and absorption spectra of iron complexes.[11b–d] In the lowest-energy calculated structure of the unsubstituted oxo complex $PcFe^{IV}{=}O(Cl)$ (Fig. 3), the Fe=O bond length of 1.674 Å was obtained. The orbitals manifold also resembles

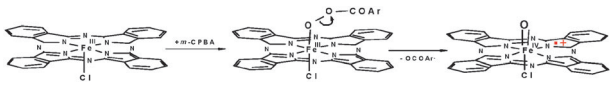

Scheme 1 Proposed mechanism for the formation of high-valent iron oxo phthalocyanine cation radical species. ^{t}Bu substituents are omitted.

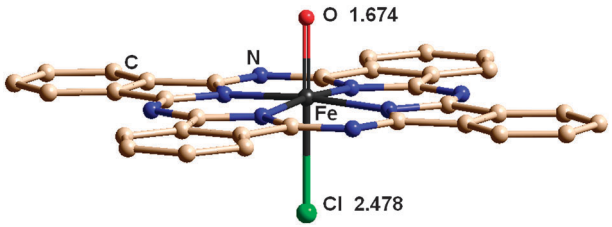

Fig. 3 DFT-optimized structure of the oxo-complex. The distances from iron centre to axial ligands are indicated. Hydrogen atoms are not shown.

the results of previous calculations for similar porphyrin and non-heme Fe(IV) oxo-complexes. The t_{2g}-set contains a non-bonding, doubly occupied (d_{xy})-based orbital and two singly occupied ($d_{xz,yz}$)-based orbitals, which are antibonding with oxygen $p_{x,y}$ orbitals. Depending on the spin state, the $d_{xy}/(d_{xz,yz})$ splitting is of 0.7–1 eV, in agreement with previous calculations of similar Fe(IV) oxo-species.[11e–g] The HOMO single occupied alpha orbital is close to the $d_{xz,yz}$ ones and contains conjugated π-orbitals of the macrocycle without substantial contribution from iron. The empty e_g-based orbitals are ($d_{x^2-y^2}$)-based π-antibonding with the equatorial ligands lying 2.9 eV above the HOMO and a 3.18 eV higher-lying (d_{z^2})-based orbital, sigma-antibonding with the oxo group (Fig. S10, ESI‡).

According to the DFT optimization, introduction of an oxygen leads to a shift of the iron atom into the plane of the Pc ring (in the initial PcFeCl complex the Fe atom is out of plane by 0.3 Å). At the same time introduction of a strong π-base oxygen ligand leads to the Fe–Cl distance lengthening from 2.32 Å in the initial complex to 2.45 Å in the oxo complex. Comparison of the calculated ground state energies of the structures with different values of spin suggests that the most energetically favourable structure contains an iron centre with S = 1 and an antiferromagnetically coupled unpaired electron on the Pc ligand. In agreement with this result, the effective spin of $\frac{1}{2}$ was observed using EPR at 120 K. To further address the spin state of iron in the complex, a high-resolution X-ray emission (XES) study was performed. $(Pc^tBu_4)FeCl$, taken as reference, shows well separated Kβ′ and $K\beta_{1,3}$ lines, typical for the high and intermediate S = 5/2 and S = 3/2 configurations.[11h] Comparison of the $(Pc^tBu_4)FeCl$ spectrum to that of the oxo complex $(Pc^tBu_4)Fe{=}O(Cl)$ (Fig. S12, ESI‡) shows a 1.0 eV decrease in energy which may be attributed to the decrease of the spin value of the latter species. At the same time the Kβ′ feature merges with the main $K\beta_{1,3}$ line, as is characteristic of the low spin-states (S = 1).[7c]

Fe K edge X-ray absorption spectroscopy supported by DFT calculations provides further evidence for the formation of

high valent iron oxo species. In the XANES spectrum, the initial (Pc^{t}Bu$_4$)FeCl complex shows a pre-edge feature at 7112.6 eV with an area of 8 arbitrary units (represented as % of the Fe K edge height[6a]). The pre-edge feature arises from 1s-to-3d transitions, the intensities of which reflect deviations of the metal center from centrosymmetry and the degree of mixing of ligand *p*-orbitals with the 3d levels of iron.[11g] Formation of oxo species leads to a shift of the pre-edge centroid to 7113.4 eV (compatible with Fe(IV) state) and an increase of area to 11 arbitrary units.

Multiple scattering simulations with FEFF code as well as time dependent DFT calculations predict a shift of the pre-edge to higher energy by a value of 1 eV upon oxidation of Fe(III) to Fe(IV). As with intensity, introduction of an additional oxygen ligand leads to a partial symmetrisation of iron coordination, from a square pyramid to a distorted octahedron, which should lead to a decrease of the pre-edge peak. However a short Fe=O bond is introduced which leads to a stronger overlap of the ligand with the 3d orbitals of iron and therefore should increase the pre-edge intensity. TD DFT calculations predict the resulting effect from these opposite contributions to be an increase of the pre-edge intensity by a factor of two. At the same time *X*- and *Y*-components of pre-edge intensity significant in the initial FePcCl disappear due to symmetrization in the *XY*-plane and the intensity of the oxo complex signal becomes totally related to the *Z*-component.

DFT-optimized structures were used to simulate EXAFS spectra and to compare them to the observed patterns. Note that direct fitting of the position and number of light ligands in such complexes seems prohibitively unreliable. Even if good figures of merit can be easily obtained by adjusting Debye–Waller factors, the reliability of such results remains questionable. Indeed, introduction of an oxygen ligand leads to complex and indirect effects on the EXAFS spectra. The scattering from the oxygen ligand placed at a short distance interferes with the scattered waves from phthalocyanine ring nitrogens, and the sign of this interference strongly depends on the relative Fe–O and Fe–N distances, making the fitting results unstable. At the same time the intensity of multiple scattering is significantly changed since the N–Fe–N angles are perturbed by the introduction of a new oxygen ligand. However, simulated EXAFS on the basis of geometry provided by the DFT-optimized structures qualitatively reproduces the experimental spectra of the starting and oxo complexes and the observed differences between them (Fig. S13, ESI‡). Thus, EXAFS results agree with DFT-optimized structure of (Pc^{t}Bu$_4^+$)Fe^{IV}=O(Cl) species (Fig. 3).

In conclusion, this work represents the first identification and characterization of the high-valent iron phthalocyanine based oxo species formulated as low spin Fe^{IV} (S = 1) antiferromagetically coupled with a phthalocyanine cation radical. The results provide a rationale for the application of the accessible iron phthalocyanine complexes in catalytic oxidation.

This work was supported by grant ANR-08-BLAN-0183-01 from Agence Nationale de la Recherche (ANR, France). We thank the Synchrotron Soleil (SAMBA beamline, Gif-sur-Yvette, France) and European Synchrotron Radiation Facility (ID26 beamline Grenoble, France) for provision of synchrotron radiation facilities. We thank Dr J. C. Swarbrick and Dr M. Rovezzi for technical assistance.

Notes and references

1 (*a*) In *Phthalocyanines Properties and Applications*, ed. C. C. Leznoff and A. B. P. Lever, VCH, New York, 1989–1996, vol. 1–4; (*b*) E. A. Lukyanets and V. N. Nemykin, *J. Porphyrins Phthalocyanines*, 2010, **14**, 1–40; (*c*) F. Dumoulin, M. Durmus and V. Ahsen, *Coord. Chem. Rev.*, 2010, **254**, 2792–2847; (*d*) J. H. Zagal, S. Griveau, J. F. Silva, T. Nyokong and F. Bedioui, *Coord. Chem. Rev.*, 2010, **254**, 2755–2791.

2 (*a*) A. B. Sorokin and E. V. Kudrik, *Catal. Today*, 2011, **159**, 37–46; (*b*) R. F. Parton, I. F. J. Vankelecom, M. J. A. Casselman, C. P. Bezoukhanova, J. B. Uytterhoeven and P. A. Jacobs, *Nature*, 1994, **370**, 541–544; (*c*) N. Sehlothi and T. Nyokong, *J. Mol. Catal. A: Chem.*, 2004, **209**, 51–57; (*d*) A. Sorokin, J.-L. Séris and B. Meunier, *Science*, 1995, **268**, 1163–1166; (*e*) O. V. Zalomaeva, I. D. Ivanchikova, O. A. Kholdeeva and A. B. Sorokin, *New J. Chem.*, 2009, **33**, 1031–1037; (*f*) C. Pérollier, C. Pergrale-Mejean and A. B. Sorokin, *New J. Chem.*, 2005, **29**, 1400–1403; (*g*) O. V. Zalomaeva and A. B. Sorokin, *New J. Chem.*, 2006, **30**, 1768–1773; (*h*) H. M. Neu, V. V. Zhdankin and V. N. Nemykin, *Tetrahedron Lett.*, 2010, **51**, 6545–6548.

3 B. Basu, S. Satapathy and A. K. Bhatnagar, *Catal. Rev.*, 1993, **35**, 571–609.

4 (*a*) J. T. Groves, R. C. Haushalter, M. Nakamura, T. E. Nemo and B. J. Evans, *J. Am. Chem. Soc.*, 1981, **103**, 2884–2886; (*b*) A. Gold, K. Jayaraj, P. Doppelt, R. Weiss, G. Chottard, E. Bill, X. Ding and A. X. Trautwein, *J. Am. Chem. Soc.*, 1988, **110**, 5756–5761; (*c*) T. Wolter, W. Meyer-Klaucke, M. Müther, D. Mandon, H. Winkler, A. X. Trautwein and R. Weiss, *J. Inorg. Biochem.*, 2000, **78**, 117–122; (*d*) A. Franke, C. Fertinger and R. van Eldik, *Angew.Chem., Int. Ed.*, 2008, **47**, 5238–5242.

5 (*a*) D. N. Harischandra, R. Zhang and M. Newcomb, *J. Am. Chem. Soc.*, 2005, **127**, 13776–13777; (*b*) A. J. McGown, W. D. Kerber, H. Fujii and D. P. Goldberg, *J. Am. Chem. Soc.*, 2009, **131**, 8040–8048.

6 (*a*) J.-U. Rohde, J.-H. In, M. H. Lim, W. W. Brennessel, M. R. Bukowski, A. Stubna, E. Münck, W. Nam and L. Que, Jr., *Science*, 2003, **299**, 1037–1039; (*b*) M. R. Bukowski, K. D. Koehntop, A. Stubna, E. L. Bominaar, J. A. Halten, E. Münck, W. Nam and L. Que, Jr., *Science*, 2005, **310**, 1000–1002; (*c*) F. Tiago de Oliveira, A. Chanda, D. Banerjee, X. Shan, S. Mondal, L. Que, Jr., E. L. Bominaar, E. Münck and T. J. Collins, *Science*, 2007, **315**, 835–838; (*d*) A. Thibon, J. England, M. Martinho, V. G. Young, J. R. Frisch, R. Guillot, J.-J. Girerd, E. Münck, L. Que, Jr. and F. Banse, *Angew. Chem., Int. Ed.*, 2008, **47**, 7064–7067; (*e*) I. Prat, J. S. Mathieson, M. Güell, X. Ribas, J. M. Luis, L. Cronin and M. Costas, *Nat. Chem.*, 2011, **3**, 788–793; (*f*) O. Y. Lyakin, K. P. Bryliakov and E. P. Talsi, *Inorg. Chem.*, 2011, **50**, 5526–5538.

7 (*a*) P. Afanasiev, E. V. Kudrik, J.-M. M. Millet, D. Bouchu and A. B. Sorokin, *Dalton Trans.*, 2011, **40**, 701–710; (*b*) A. B. Sorokin, E. V. Kudrik and D. Bouchu, *Chem. Commun.*, 2008, 2562–2564; (*c*) E. V. Kudrik, O. Safonova, P. Glatzel, J. C. Swarbrick, L. X. Alvarez, A. B. Sorokin and P. Afanasiev, *Appl. Catal., B*, 2012, **113–114**, 43–51; (*d*) P. Afanasiev, D. Bouchu, E. V. Kudrik, J.-M. M. Millet and A. B. Sorokin, *Dalton Trans.*, 2009, 9828–9836; (*e*) E. V. Kudrik and A. B. Sorokin, *Chem.–Eur. J.*, 2008, **14**, 7123–7126.

8 J. Rittle and M. T. Green, *Science*, 2010, **330**, 933–937.

9 (*a*) E. Ough, Z. Gasyna and M. J. Stillman, *Inorg. Chem.*, 1991, **30**, 301–310; (*b*) T. Nyokong, Z. Gasyna and M. J. Stillman, *Inorg. Chem.*, 1987, **26**, 547–553.

10 J. Bernadou and B. Meunier, *Chem. Commun.*, 1998, 2167–2173.

11 (*a*) F. Neese, *ORCA, an Ab Initio Density Functional and Semiempirical Electronic Structure Program Package, version 2.8*, Universität Bonn, Germany, 2011; (*b*) F. Neese, *Inorg. Chim. Acta*, 2002, **337**, 181–192; (*c*) T. A. Jackson, J.-U. Rohde, M. S. Seo, C. V. Sastri, R. DeHont, A. Stubna, T. Ohta, T. Kitagawa, E. Münck, W. Nam and L. Que, Jr., *J. Am. Chem. Soc.*, 2008, **130**, 12394–12407; (*d*) P. Chandrasekaran, S. Chantal, E. Stieber, T. J. Collins, L. Que and F. Neese, *Dalton Trans.*, 2011, **40**, 11070–11079; (*e*) H. Hirao, S. Shaik and P. M. Kozlowski, *J. Phys. Chem. A*, 2006, **110**, 6091–6099; (*f*) S. Shaik, D. Kumar, S. P. de Visser, A. Altun and W. Thiel, *Chem. Rev.*, 2005, **105**, 2279–2338; (*g*) T. E. Westre, P. Kennepohl, J. G. DeWitt, B. Hedman, K. O. Hodgson and E. I. Solomon, *J. Am. Chem. Soc.*, 1997, **119**, 6297–6314; (*h*) P. Glatzel and U. Bergmann, *Coord. Chem. Rev.*, 2005, **249**, 65–95.

